Supporting Information

One-pot Synthesis of Manganese Oxides and Cobalt Phosphides Nanohybrids with Abundant Hetero-interfaces in Amorphous Matrix for Efficient Hydrogen Evolution in Alkaline Solution

Dan Zhou‡[a,b], Zheng Wang‡[a], Xia Long[a], Yiming An[b], He Lin[b], Zheng Xing[b], Ming Ma[b], Shihe Yang[a,b]*

[a] Guangdong Key Lab of Nano-Micro Material Research, School of Chemical Biology and Biotechnology, Peking University Shenzhen Graduate School, Shenzhen, China

[b] Department of Chemistry, The Hong Kong University of Science and Technology, Clear Water Bay, Kowloon, Hong Kong, China

‡ Dan Zhou and Zheng Wang contributed equally to this work.

Experimental Section

Materials

$CoCl_2 \cdot 6H_2O$, $Mn(NO_3)_2$, NaH_2PO_2, KOH were purchased from Sigma-Aldrich. All chemicals were of analytical grade and were used without further purification. Ultrapure deionized water (18.2 MΩ/cm) was used in all experiments.

Experimental methods

Carbon cloth substrates were consecutively washed with acetone and deionized water under ultrasonication for 30 minutes in each solution to thoroughly remove impurities. Then, the as cleaned carbon cloth was further oxidized in concentrated nitric acid by hydrothermal reaction at 110 ℃ for 6 hours. The as obtained oxidized carbon cloth (denoted as CC) was further thoroughly cleaned with deionized water. As a result, the hydrophobic carbon cloth became hydrophilic.

In a typical synthesis, a three-electrode system was used for electrodeposition with CC (1×2 cm^2) as the work electrode, Ag/AgCl (saturated KCl solution) as the reference electrode and carbon rod as the counter electrode. The electrolyte for electrodeposition of manganese and cobalt layered double hydroxide (MnCo-LDH)

was freshly prepared by dissolving total amount 1.2 mmol of $CoCl_2 \cdot 6H_2O$ and $Mn(NO_3)_2$ (Co/Mn molar ratios were set as 9:1, 8:2, 7:3, 6:4, 5:5 and 3:7 for comparison to find an optimized composition) in 20 mL deionized water. The potentiostatic deposition was carried out at a potential of -1.1 V vs. Ag/AgCl for 100 seconds. The resulting MnCo-LDH nanosheets array supported on carbon cloth (denoted as MnCo-LDH/CC) was rinsed with deionized water and ethanol and then dried in air at room temperature.

Before phosphorization, MnCo-LDH/CC was annealed in a furnace by heating up to 300 ℃ with ramping rate of 5 ℃/min and maintained at 300 ℃ for 2 h. Then, the as-obtained MnCo-O/CC was put in a quartz boat and placed at the center of the quartz tube, and 1.0 g Na_2HPO_2 was loaded into another quartz boat and placed at the upstream of the quartz tube with a distance of 2 cm from MnCo-O/CC. After flushing with high-purity argon thoroughly, the tube was heated from room temperature to 350 ℃ with a ramping rate of 2 ℃/min and maintained at that temperature for 2 h. Then it was naturally cooled down to room temperature in a continuous argon flow. The as obtained integrated manganese oxide and cobalt phosphide nanohybrids nanosheets array supported on carbon cloth (denoted as Mn-O@Co-P/CC) was washed with water and ethanol and then dried in air at room temperature.

For comparison, $Co(OH)_2$/CC and Co-P/CC were prepared with the same procedure without manganese source inputting. $Mn(OH)_2$ and Mn-O/CC were prepared with the same procedure without cobalt source inputting. Cobalt phosphide covered with a layer of manganese oxide supported on carbon cloth (Mn-O/Co-P/CC) was prepared by electrodepositing a layer of $Mn(OH)_2$ (20s) on previously electrodeposited $Co(OH)_2$ (80s) and following the same annealing and phosphorization processes.

Materials Characterization

The morphology of the as synthesized samples was characterized by scanning electron microscopy (SEM) on JEOL 7100F at an accelerating voltage of 10 kV. The phase structure was determined by X-ray diffraction (XRD) which was carried out on a Philips PW-1830 X-ray diffractometer with Cu Kα radiation (K=0.15418 nm). Transmission electron microscope (TEM), high resolution transmission electron microscope (HRTEM) and energy-disperse X-ray spectrum (EDX) were taken on JEOL-

2010 with an acceleration voltage of 200 kV. X-ray photoelectron spectroscopy (XPS) were measured on a Perkin-Elmer model PHI 5600 XPS system with a resolution of 0.3–0.5 eV from a monochromated aluminum anode X-ray source with Mo Kα radiation (1486.6 eV).

Electrochemical Measurements

The as prepared catalysts supported on carbon cloth were directly used as work electrodes. All electrochemical characterizations were performed with CHI 660D electrochemistry workstation (Shanghai Chenhua Instrument, Inc.) using a standard three-electrode electrochemical cell with Hg/HgO (1.0 M NaOH) electrode and carbon rod as reference and counter electrode, respectively. Electrochemically inert tape was used to define the 0.5 cm^2 electrode area. The electrochemical measurements were all performed at room temperature, and the potential was referenced to reversible hydrogen electrode (RHE). The calculate equation is: E (vs. RHE) = E (vs. Hg/HgO) + $E_{Hg/HgO}$ (vs. RHE). For the RHE calibration of Hg/HgO reference electrode, the potential difference between Hg/HgO and RHE was measured in a cell where Pt foil was used as the working electrode and Hg/HgO was used as the counter and reference electrodes in a 99.999% pure H_2-saturated 1.0 M KOH aqueous solution. 1.0 M KOH (pH 14) was prepared as electrolyte. Cyclic voltammogram (CV) scans at a scan rate of 50 mV s^{-1} between 0 to -0.5 V vs. RHE. were taken several cycles to bubble away the surface contaminates and at the same time stabilize the catalysts. Linear sweep voltammograms (LSV) measurements were recorded at a scan rate of 5 mV/s and converted to RHE scale. 95% iR compensation was applied for all polarization curves. All chronopotentiometry curves were shown without iR compensation. Electrochemical impedance spectroscopy (EIS) was carried at -0.1 V vs. RHE over a frequency range from 1 MHz to 0.1 Hz with a 5 mV AC dither.

Density functional theory calculations

All the first-principles spin-polarized calculations were performed using Vienna ab initio simulation package (VASP).[1,2] Projector augmented wave (PAW) potentials were employed to describe the core-valance interactions.[3] The generalized gradient approximation with the Perdew, Burke, and Ernzerhof (PBE) functional[4] was employed to treat the electronic exchange and correlation. The energy cutoff for the plane-wave

basis set is set as 500 eV. The convergence criteria is set as 0.01 eV/Å for maximal forces and 10^{-4} eV for energies. The Gibbs free energy ΔG_i *(i=1,2,3,4,5)* is calculated by $\Delta G_i = \Delta E_i + \Delta ZPE - T\Delta S$ with T set as 298 K. The free energy of $H^+ + e$ is set as zero at an electrode potential of U=0, the zero point energy and entropy is set as 0.27 eV and 0.41 eV, respectively.[5] All the structures are shown by VESTA.[6]

(002) surface of Co_2P with a chemical formula of $Co_{24}P_{12}$ was chosen for the study of HER activity of Co_2P, the bottom layer of Co_2P was fixed during the calculations. For the Co-P/Mn-O interface, we first separately build the (002) surfaces of Co_2P and Mn_3O_4, respectively. For the (002) surface of Mn_3O_4, hydrogen was employed to passivate the surface. Then, we cleave the (010) surfaces of Co_2P and Mn_3O_4, and combine them together along the newly cleaved (010) surfaces to obtain the Mn-O@Co-P interface. The interface has a chemical formual of $Co_{24}P_{12}Mn_{14}O_{28}H_{20}$, and the hydrogen evolution reactions are modelled on the (002) surfaces of them.

$$* + H_2O \longrightarrow H_2O* \qquad \Delta G1$$

$$H_2O* \longrightarrow OH* + H* \qquad \Delta G2$$

$$OH* + H* + H_2O + e + H^+ \longrightarrow H_2O* + H* + H_2O \qquad \Delta G3$$

$$H_2O* + H* \longrightarrow OH* + H_2 \qquad \Delta G4$$

$$OH* + e + H^+ \longrightarrow H_2O \qquad \Delta G5$$

Scheme S1. The general mechanism of hydrogen evolution reactions.

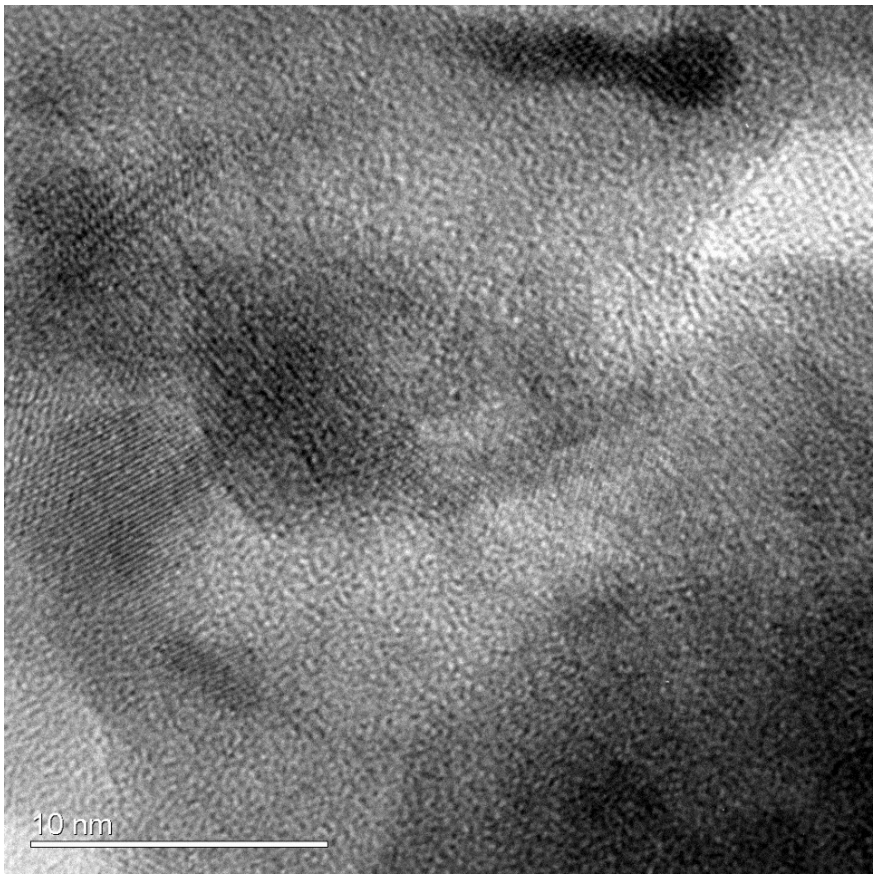

a

b

Figure S1. (a, b) HRTEM image of Mn-O@Co-P/CC.

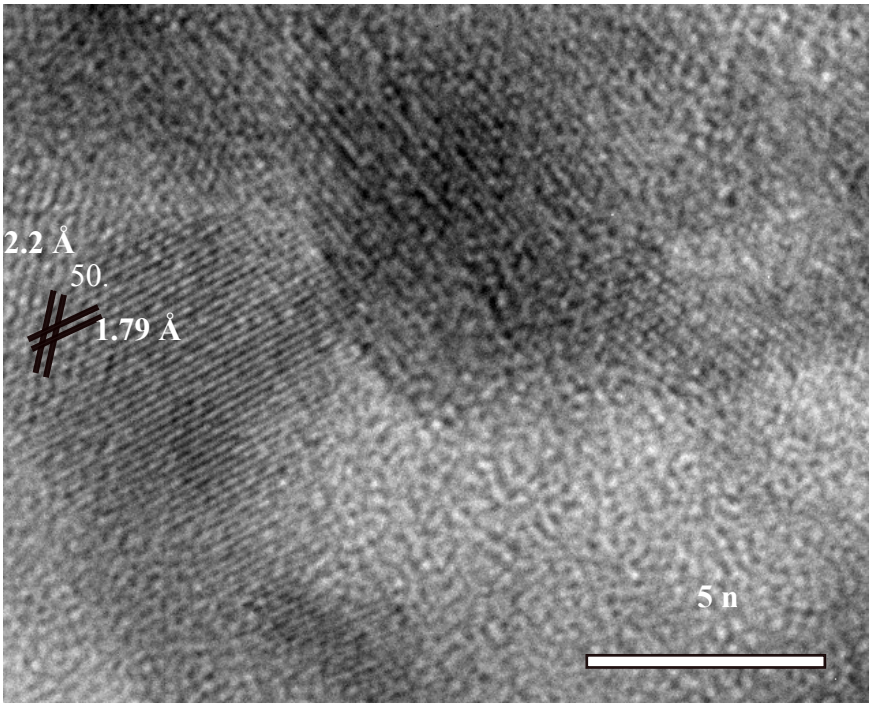

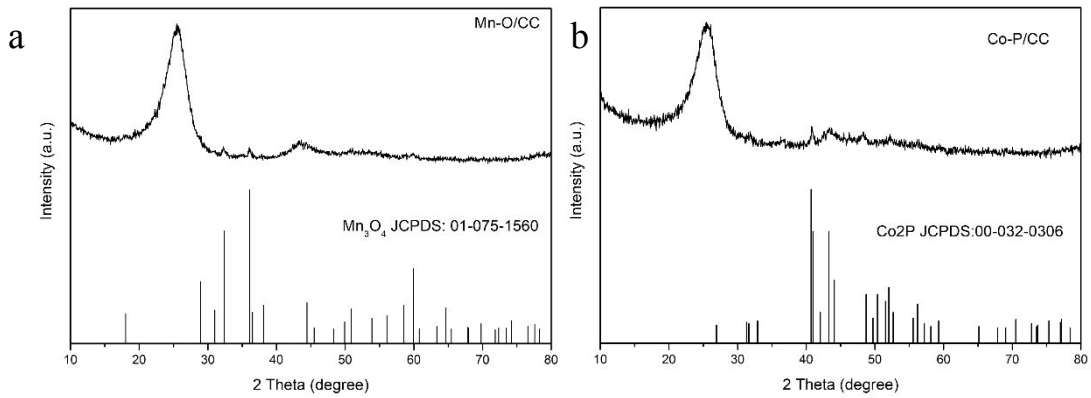

Figure S2. XRD patterns for (a) Mn-O/CC and (b) Co-P/CC.

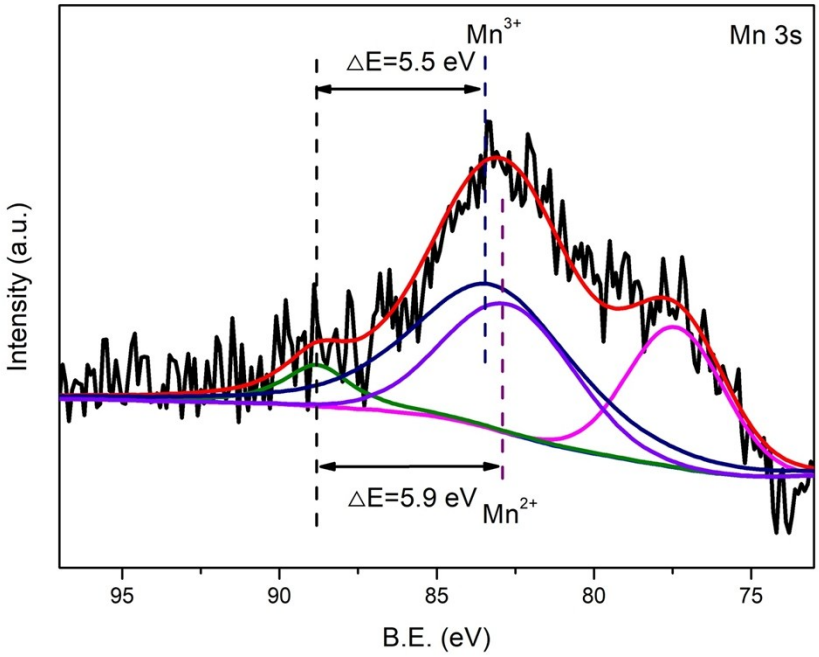

Figure S3. The high resolution XPS spectrum in the Mn 3s region.

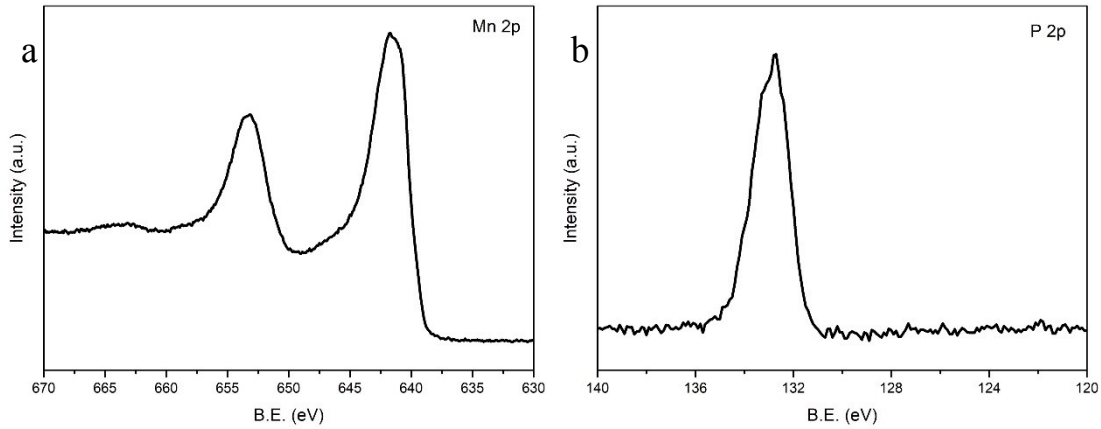

Figure S4. High resolution XPS spectra of (a) Mn 2p and (b) P 2p of Mn-O/CC.

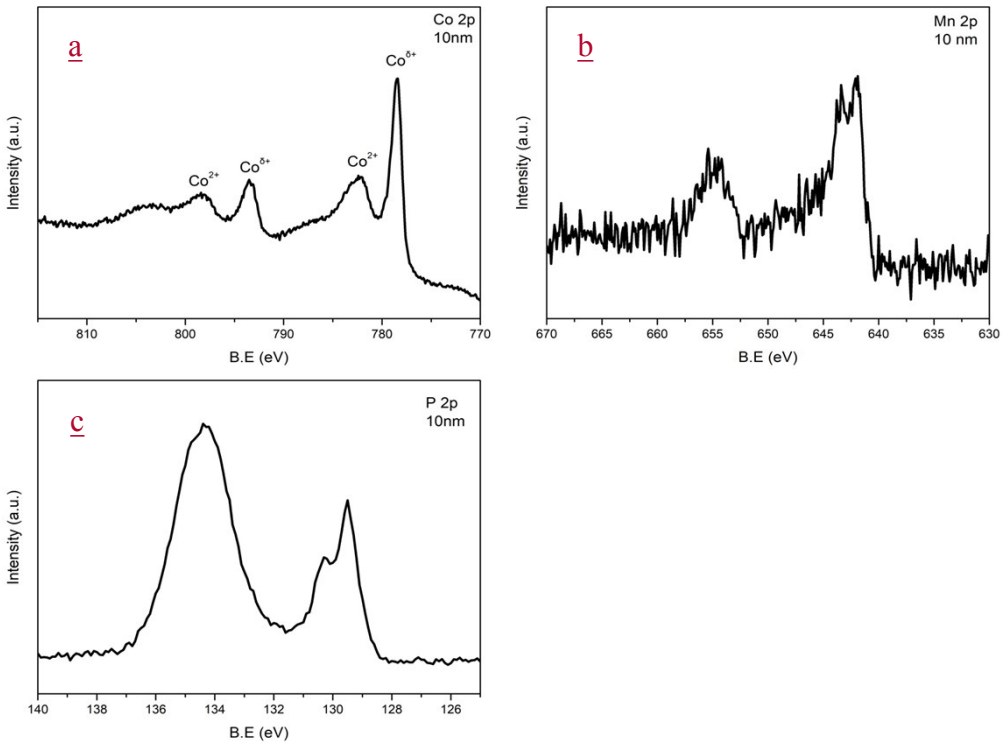

Figure S5. High resolution depth XPS spectra (Sputtered by Ar for 130s) of Mn-O@Co-P in the (a) Co 2p, (b) Mn 2p and (c) P 2p regions.

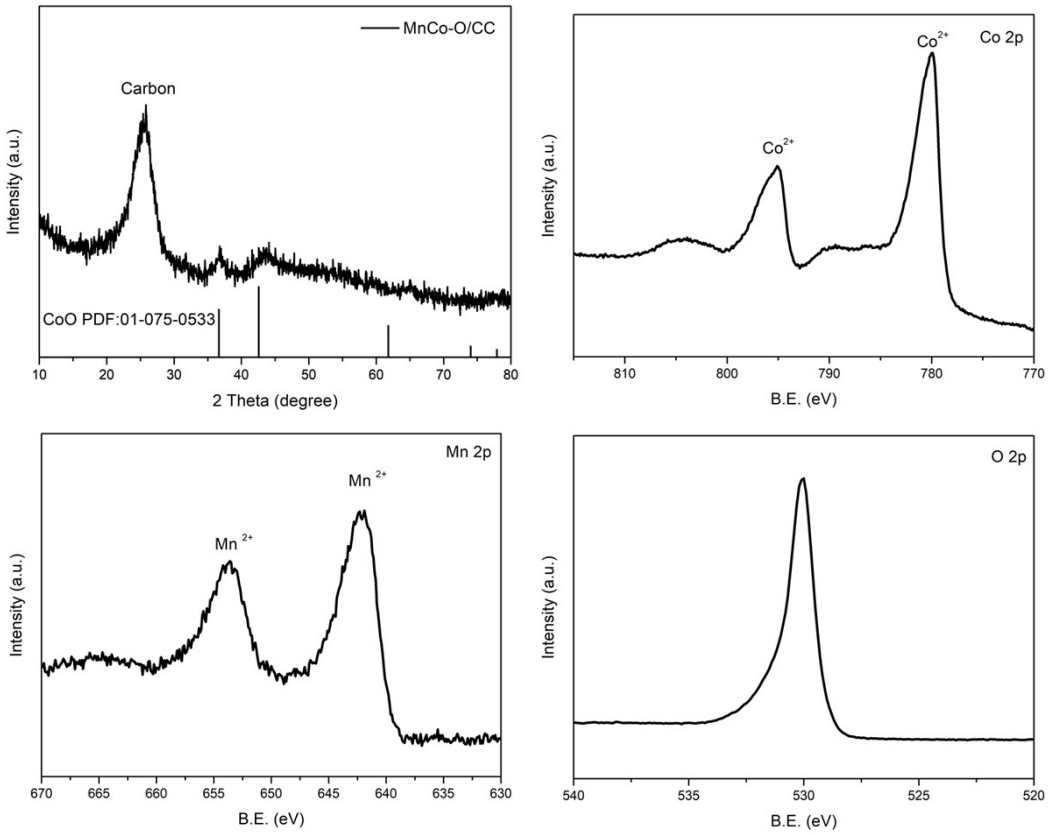

Figure S6. (a) XRD patterns of MnCo-O/CC. High resolution XPS spectra in the (b) Co 2p, (c) P 2p and (d) Mn 2p regions.

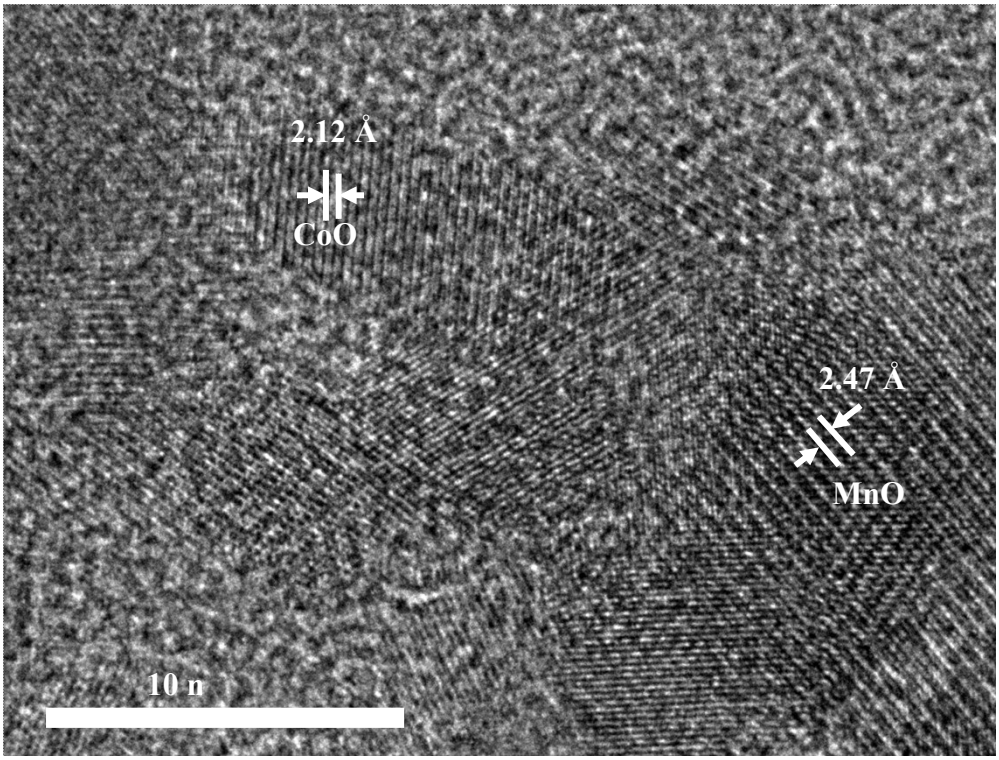

Figure S7. HRTEM image of MnCo-O/CC.

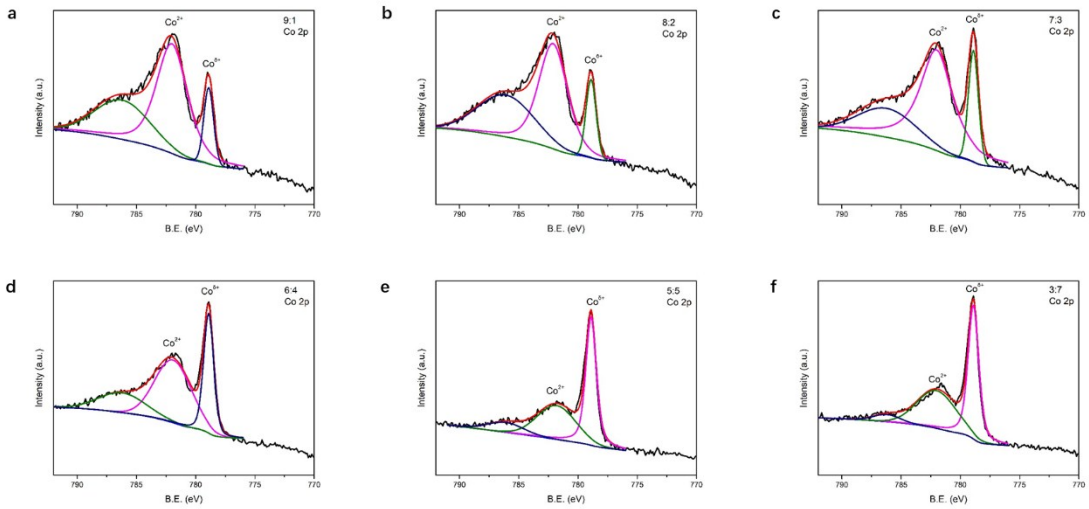

Figure S8. High resolution XPS spectra of Co 2p for Mn-O@Co-P/CC with initial Co:Mn ratio of (a) 9:1, (b) 8:2 (c) 7:3, (d) 6:4, (e) 5:5, (f) 3:7.

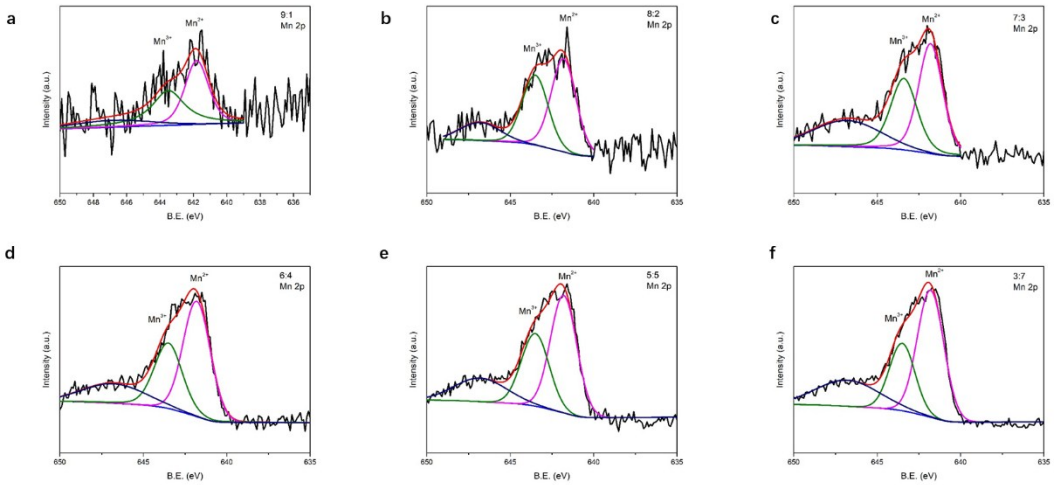

Figure S9. High resolution XPS spectra of Mn 2p for Mn-O@Co-P/CC with initial Co:Mn ratio of (a) 9:1, (b) 8:2 (c) 7:3, (d) 6:4, (e) 5:5, (f) 3:7.

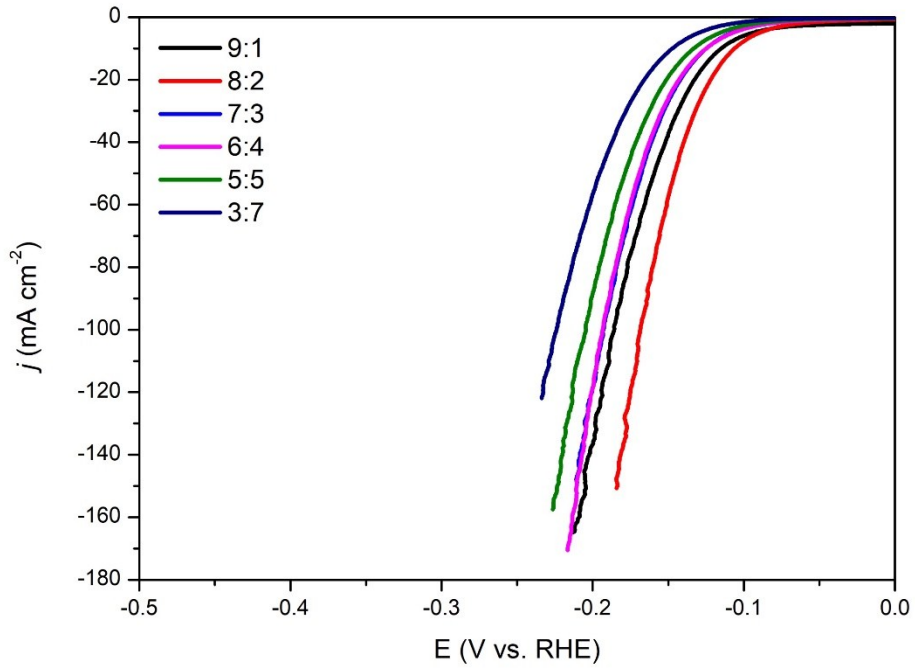

Figure S10. LSV curves of Mn-O@Co-P/CC as a function of initial Co/Mn ratio.

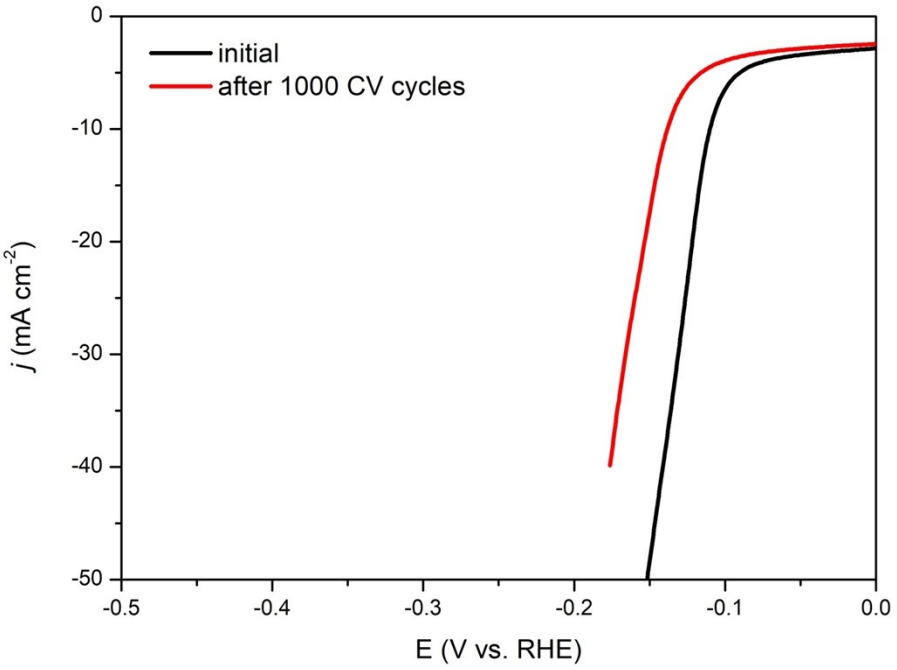

Figure S11. Polarization curves before and after 10000 CV cycles of Mn-O@Co-P/CC ranging from −0.18 to 0 V.

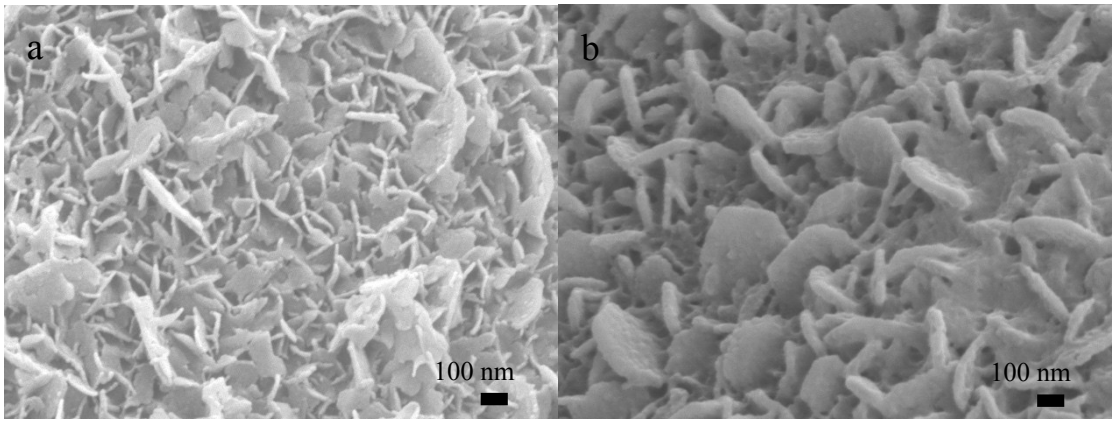

Figure S12. SEM images of (a) $Mn(OH)_2/Co(OH)_2$/CC and (b) Mn-O/Co-P/CC.

$2Co + O_2 \rightarrow 2CoO$	(S1)	ΔE= -2.32 eV
$2Mn + O_2 \rightarrow 2MnO$	(S2)	ΔE= -4.95 eV
$Co + P \rightarrow CoP$	(S3)	ΔE= -1.17 eV
$2Co + P \rightarrow Co_2P$	(S4)	ΔE= -1.52 eV
$Mn + P \rightarrow MnP$	(S5)	ΔE= -1.32 eV
$2Mn + P \rightarrow Mn_2P$	(S6)	ΔE= -1.71 eV

Scheme S2: The calculated reaction energies of formation of CoO, MnO, CoP, Co_2P, MnP and Mn_2P, respectively.

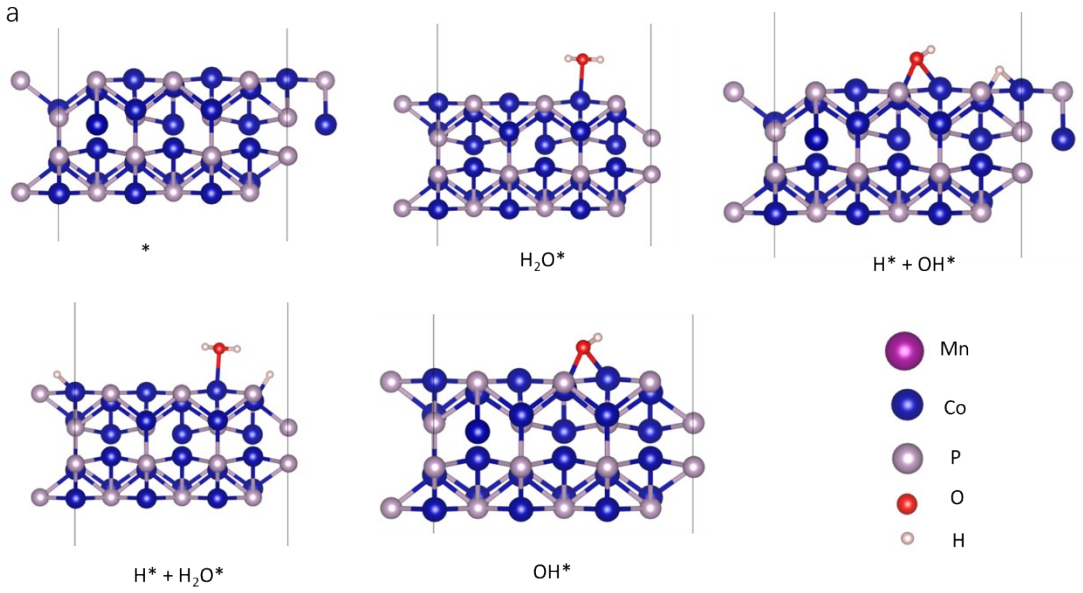

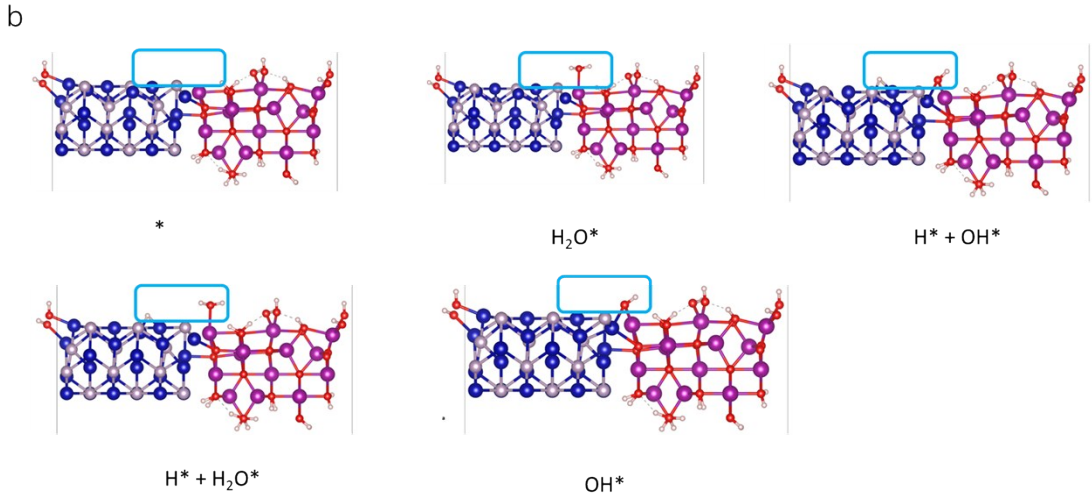

Figure S13. The structures of key intermediate: *, H_2O*, H* + OH*, H* + H_2O* and OH* for (a) Co_2P (b) Co_2P-Mn_3O_4.

Table S1. The mass loading of Mn-O@Co-P on carbon cloth.

	Sample 1	Sample 2	Sample 3	Average
Mass loading mg/cm^2	0.92	0.99	1.03	0.98

Table S2. The atomic percent of each element in Mn-O@Co-P/CC.

Element	Co	P	Mn	O	Total
Atomic%	22.87	40.85	2.47	33.81	100

Table S3. $Co^{\delta+}/Co^{2+}$ and Mn^{3+}/Mn^{2+} molar ratio of Mn-O@Co-P with an initial Co:Mn ratio of 9:1, 8:2, 7:3, 6:4, 3:7.

Co/Mn	$Co^{\delta+}/Co^{2+}$	Mn^{3+}/Mn^{2+}
9:1	0.181	0.940
8:2	0.228	0.764
7:3	0.246	0.733
6:4	0.592	0.623
3:7	1.189	0.512

Table S4. Comparison of HER catalytic performance in alkaline condition. (1M KOH solution)

Catalyst	Substrate	Overpotential at 10 mA cm-2 (mV)	Tafel slope (mV dec^{-1})	References
CoP encapsulated in B,N doped nanotubes	glassy carbon	215	52	Tabassum et al.[7]
N-doped carbon coated CoP	N-doped graphene	155	68.6	Ma et al. [8]
Co_2P quantum dots embedded in N, P dual-doped carbon	carbon cloth	129	93	Zhang et al.[9]
CoPS	N-doped carbon matrix	148	78	Li et. al.[10]
O-Co_2P	rotating disk electrode	160	61.1	Xu et al.[11]
Ni_2P/CoP	carbon cloth	73	120	Wang et al.[12]
Co/CoP	N-doped nanoporous carbon membranes	135	64	Wang et al.[13]
NiCoP	glassy carbon	124	42	Li et al.[14]
Mn-doped CoP	carbon rod	95	-	Li et.al.[15]
Mn-doped CoP_3	carbon fiber	96	60	Feng et al.[16]
Fe-doped CoP	Ti foil	78	75	Tang et. al.[17]
Mn-doped CoP	Ti mesh	76	52	Liu et al.[18]
Mo-doped CoP	carbon cloth	49	80	Liu et al.[19]
Mn-O@CoP	carbon cloth	106	56	This work

References:

1. Kresse, G.; Furthmüller J., Efficiency of ab-initio total energy calculations for metals and semiconductors using a plane-wave basis set. *Comp. Mater. Sci.* **1996**, *6* (1), 15-50.

2. Kresse, G.; Furthmüller J., Efficient iterative schemes for ab initio total-energy calculations using a plane-wave basis set. *Phys. Rev. B* **1996**, *54* (16), 11169-11186.

3. Blöchl, P. E., Projector augmented-wave method. *Phys. Rev. B* **1994**, *50* (24), 17953-17979.

4. Perdew, John P.; Burke Kieron; Ernzerhof Matthias, Generalized Gradient Approximation Made Simple. *Phys. Rev. Lett.* **1996**, *77* (18), 3865-3868.

5. Rossmeisl, J.; Logadottir A.; Nørskov J. K., Electrolysis of water on (oxidized) metal surfaces. *Chem. Phys.* **2005**, *319* (1), 178-184.

6. Momma, Koichi; Izumi Fujio, VESTA 3 for three-dimensional visualization of crystal, volumetric and morphology data. *J. Appl. Crystallography* **2011**, *44* (6), 1272-1276.

7. Tabassum, Hassina; Guo Wenhan; Meng Wei; Mahmood Asif; Zhao Ruo; Wang Qingfei; Zou Ruqiang, Metal–Organic Frameworks Derived Cobalt Phosphide Architecture Encapsulated into B/N Co-Doped Graphene Nanotubes for All pH Value Electrochemical Hydrogen Evolution. *Adv. Energy Mater.* **2017**, *7* (9), 1601671.

8. Ma, Jingwen; Wang Min; Lei Guangyu; Zhang Guoliang; Zhang Fengbao; Peng Wenchao; Fan Xiaobin; Li Yang, Polyaniline Derived N-Doped Carbon-Coated Cobalt Phosphide Nanoparticles Deposited on N-Doped Graphene as an Efficient Electrocatalyst for Hydrogen Evolution Reaction. *Small* **2018**, *14* (2), 1702895.

9. Zhang, Chengtian; Pu Zonghua; Amiinu Ibrahim Saana; Zhao Yufeng; Zhu Jiawei; Tang Yongfu; Mu Shichun, Co2P quantum dot embedded N, P dual-doped carbon self-supported electrodes with flexible and binder-free properties for efficient hydrogen evolution reactions. *Nanoscale* **2018**, *10* (6), 2902-2907.

10. Li, Yuzhi; Niu Siqi; Rakov Dmitrii; Wang Ying; Cabán-Acevedo Miguel; Zheng Shijian; Song Bo; Xu Ping, Metal organic framework-derived CoPS/N-doped carbon for efficient electrocatalytic hydrogen evolution. *Nanoscale* **2018**, *10* (15), 7291-7297.

11. Xu, Kun; Ding Hui; Zhang Mengxing; Chen Min; Hao Zikai; Zhang Lidong; Wu Changzheng; Xie Yi, Regulating Water-Reduction Kinetics in Cobalt Phosphide for Enhancing HER Catalytic Activity in Alkaline Solution. *Adv. Mater.* **2017**, *29* (28),

1606980.

12. Wang, An-Liang; Lin Jing; Xu Han; Tong Ye-Xiang; Li Gao-Ren, Ni2P–CoP hybrid nanosheet arrays supported on carbon cloth as an efficient flexible cathode for hydrogen evolution. *J. Mater. Chem. A* **2016**, *4* (43), 16992-16999.

13. Wang, Hong; Min Shixiong; Wang Qiang; Li Debao; Casillas Gilberto; Ma Chun; Li Yangyang; Liu Zhixiong; Li Lain-Jong; Yuan Jiayin; Antonietti Markus; Wu Tom, Nitrogen-Doped Nanoporous Carbon Membranes with Co/CoP Janus-Type Nanocrystals as Hydrogen Evolution Electrode in Both Acidic and Alkaline Environments. *ACS Nano* **2017**, *11* (4), 4358-4364.

14. Li, Yapeng; Liu Jindou; Chen Chen; Zhang Xiaohua; Chen Jinhua, Preparation of NiCoP Hollow Quasi-Polyhedra and Their Electrocatalytic Properties for Hydrogen Evolution in Alkaline Solution. *ACS Appl. Mater. Interfaces* **2017**, *9* (7), 5982-5991.

15. Li, Xiumin; Li Shasha; Yoshida Akihiro; Sirisomboonchai Suchada; Tang Keyong; Zuo Zhijun; Hao Xiaogang; Abudula Abuliti; Guan Guoqing, Mn doped CoP nanoparticle clusters: an efficient electrocatalyst for hydrogen evolution reaction. *Catal. Sci. Technol.* **2018**, *8* (17), 4407-4412.

16. Feng, Jiajia; Wang Xiaodeng; Zhang Dingke; Wang Yue; Wang Jing; Pi Mingyu; Zhou Hongpeng; Li Jinhua; Chen Shijian, Porous Mn-Doped CoP3 Nanowires as a Janus Electrocatalyst for Efficient Overall Water Splitting in Alkaline Solution. *J. Electrochem. Soc.* **2018**, *165* (16), F1323-F1330.

17. Tang, Chun; Zhang Rong; Lu Wenbo; He Liangbo; Jiang Xiue; Asiri Abdullah M.; Sun Xuping, Fe-Doped CoP Nanoarray: A Monolithic Multifunctional Catalyst for Highly Efficient Hydrogen Generation. *Adv. Mater.* **2017**, *29* (2), 1602441.

18. Liu, Tingting; Ma Xiao; Liu Danni; Hao Shuai; Du Gu; Ma Yongjun; Asiri Abdullah M.; Sun Xuping; Chen Liang, Mn Doping of CoP Nanosheets Array: An Efficient Electrocatalyst for Hydrogen Evolution Reaction with Enhanced Activity at All pH Values. *ACS Catal.* **2017**, *7* (1), 98-102.

19. Liu, Xunhang; Wei Bo; Su Ren; Zhao Chenguang; Dai Dongmei; Ma Xiao; Xu Lingling, Mo-Doped Cobalt Phosphide Nanosheets for Efficient Hydrogen Generation in an Alkaline Media. *Energy Technol.* **2019**, *7* (6), 1900021.